

Structural Study of Icosahedral Al₆₅Cu₂₀TM₁₅ (TM= Fe, Ru, and Os) and Decagonal Al₇₅Fe₁₅Ni₁₀ Alloys by Anomalous X-ray Scattering((B)Quasicrystals)

著者	Matsubara Eiichiro, Waseda Yoshio
journal or publication title	Science reports of the Research Institutes, Tohoku University. Ser. A, Physics, chemistry and metallurgy
volume	36
number	1
page range	128-142
year	1991-03-25
URL	http://hdl.handle.net/10097/28371

**Structural Study of Icosahedral $\text{Al}_{65}\text{Cu}_{20}\text{TM}_{15}$ (TM= Fe, Ru, and Os)
and Decagonal $\text{Al}_{75}\text{Fe}_{15}\text{Ni}_{10}$ Alloys by Anomalous X-ray Scattering***

Eiichiro Matsubara and Yoshio Waseda

Research Institute of Mineral Dressing and Metallurgy (SENKEN)

(Received January 29, 1991)

Synopsis

The structural study has been carried out in fully annealed quasi-crystalline $\text{Al}_{65}\text{Cu}_{20}\text{TM}_{15}$ (TM=Fe, Ru and Os) and as-quenched decagonal $\text{Al}_{75}\text{Fe}_{15}\text{Ni}_{10}$ alloys by anomalous x-ray scattering (AXS) and ordinary x-ray scattering techniques. The environmental radial distribution functions (RDFs) for Cu and Os atoms in the $\text{Al}_{65}\text{Cu}_{20}\text{Os}_{15}$ alloy and those of Fe and Ni atoms in the $\text{Al}_{75}\text{Fe}_{15}\text{Ni}_{10}$ alloy were determined and compared with the ordinary RDF which represents the average structure of the system. Environmental structures for Cu and Os atoms are quite different in the $\text{Al}_{65}\text{Cu}_{20}\text{Os}_{15}$ alloy, which implies that Cu and Os atoms occupy different sites in icosahedral clusters. By comparing the ordinary RDFs of the three $\text{Al}_{65}\text{Cu}_{20}\text{TM}_{15}$ (TM=Fe, Ru and Os) alloys, their fundamental atomic structure is found to be identical. The environmental RDFs for Fe and Ni atoms in the decagonal $\text{Al}_{75}\text{Ni}_{10}\text{Fe}_{15}$ alloy resemble each other and also the ordinary RDF, which contrasts to the environmental RDFs for Cu and Os atoms in the $\text{Al}_{65}\text{Cu}_{20}\text{Os}_{15}$ alloy. These results suggest that Ni and Fe atoms share their atomic sites in the decagonal $\text{Al}_{75}\text{Fe}_{15}\text{Ni}_{10}$ structure.

I. Introduction

Tsai et al.¹⁻³) found a thermodynamically stable single icosahedral phase of $\text{Al}_{65}\text{Cu}_{20}\text{TM}_{15}$ (TM=Fe, Ru and Os) alloys in conventionally solidified and fully annealed states as well as in rapidly

* The 91-R3 report of the Research Institute of Mineral Dressing and Metallurgy (SENKEN).

quenched state. Their atomic structures observed with x-ray and electron diffraction, and high-resolution electron microscopy revealed the high degree of structural perfection. The environmental structures for Cu and Fe atoms in the as-quenched icosahedral $\text{Al}_{65}\text{Cu}_{20}\text{Fe}_{15}$ alloy indicate that the environment for Cu is quite different from that for Fe⁴⁾. Structural studies of the as-quenched and fully annealed $\text{Al}_{65}\text{Cu}_{20}\text{Fe}_{15}$ alloys by the ordinary x-ray diffraction method show some differences of their intensity profiles which appear to be attributed to defects or stains introduced during rapid quench⁴⁾.

Henley⁵⁾ classifies Al-based icosahedral alloys into two major categories, i.e. "i-(Al-M)" and "AlZnMg" classes where "M" stands for transition metals. These two kinds of icosahedral phases have different atomic structures although their fundamental structural symmetry is still an icosahedral symmetry. The present $\text{Al}_{65}\text{Cu}_{20}\text{TM}_{15}$ alloys belong to the former class. Some decagonal alloys which have a layered structure of two-dimension quasicrystals are also classified into the i(Al-M) type. Some workers have considered that the fundamental properties and the atomic structures of the decagonal phase may be the key to understanding of a three-dimensional icosahedral phase. However, most of decagonal phases have been formed as a mixture with crystalline and icosahedral phases in a narrow composition range between crystalline and icosahedral phases, which makes the characterization of physical and chemical properties and their atomic structure extremely difficult. Recently, Tsai et al.⁶⁾ reported new single decagonal phases in Al-Ni-Fe and Al-Ni-Co systems produced by rapid quench. Furthermore, in the ternary Al-Co-Cu alloy, the stable decagonal phase has been produced by conventional solidification as well as by rapid quenching⁷⁾. The discovery of such single decagonal alloys may give an important approach for characterization of not only the decagonal phase but also the icosahedral phase.

The term "quasicrystal" which is an abbreviation for "quasiperiodic crystal" describes a new type of crystalline structures which have sharp Bragg peaks but which have no long-range periodic order⁵⁾. Thus, the quasicrystal has an infinite number of sites which are not exactly equivalent, which makes construction of a structural model for a quasicrystals extremely complicate. One successful approach to the atomic structure is the "rigid geometry plus decoration" in Henley's phrase⁸⁾. While the rigid geometry in the ordinary crystals is trivial, i.e. the Bravais lattices, an example of a rigid geometry in the quasicrystal is a Penrose tiling. By placing atoms on the rigid geometrical frame with a certain decoration rule, the atomic

structure of a quasicrystal can be described. Such a decoration rule has often been inferred from a crystalline structure as Audier⁹) used the α -phase to construct the atomic structural model for the icosahedral Al-Mn-Si alloy. Local probes, e.g. the EXAFS (extended x-ray absorption fine structure) technique, the anomalous x-ray scattering (AXS) technique and the neutron diffraction technique with isotopically substituted samples, are useful experimental methods to study a decoration rule in quasicrystals. In the present study, the AXS method was applied to the fully annealed Al₆₅Cu₂₀Os₁₅ alloy and the as-quenched Al₇₅Fe₁₅Ni₁₀ alloy. The experimental results of the environmental structures for Cu and Os atoms in the Al₆₅Cu₂₀Os₁₅ alloy, and those for Fe and Ni atoms in the Al₇₅Fe₁₅Ni₁₀ alloy will be presented and discussed the atomic structure of these icosahedral, or decagonal clusters in each alloy.

II. Experimental

Ingots of Al₆₅Cu₂₀Fe₁₅, Al₆₅Cu₂₀Ru₁₅, Al₆₅Cu₂₀Os₁₅ and Al₇₅Fe₁₅Ni₁₀ were prepared by arch-melting from mixtures of high-purity (>99.7wt%) metals of Al, Cu, Fe, Ru, Os and Ni in an argon atmosphere. From these master ingots, ribbons of about 0.02mm thickness and 1mm width were prepared by a single-roller melt-spinning technique. Subsequently, the as-quenched alloys were annealed in vacuum for 172.8 ks (48 hrs) at 1073 K (0.94 T_m) for Al₆₅Cu₂₀Fe₁₅, for 172.8 ks (48 hrs) at 1090 K (0.94 T_m) for Al₆₅Cu₂₀Ru₁₅ and for 129.6 ks (36 hrs) at 1143 K (<0.76 T_m) for Al₆₅Cu₂₀Os₁₅, where T_m stands for the melting points of 1140 K, 1160 K and >1473 K in each icosahedral phase. The details of the sample preparation may be find in refs.1, 2, 3 and 6.

Ordinary x-ray scattering profiles by the Mo K α radiation of the fully annealed icosahedral Al₆₅Cu₂₀Fe₁₅, Al₆₅Cu₂₀Ru₁₅ and Al₆₅Cu₂₀Os₁₅ alloys and of the as-quenched decagonal Al₇₅Fe₁₅Ni₁₀ alloy, and anomalous x-ray scattering (AXS) profiles at Cu K- and L_{III}-absorption edges of the fully annealed icosahedral Al₆₅Cu₂₀Os₁₅ alloys and at Fe and Ni K-absorption edges of the as-quenched decagonal Al₇₅Fe₁₅Ni₁₀ alloy were measured. For these x-ray measurements, powder samples were prepared by grinding the ribbons.

The AXS measurements were carried out with synchrotron radiation at the Photon Factory of the National Laboratory for High Energy Physics, Tsukuba Japan. Since the details of the experimental setting and analysis are explained in ref.10, only some additional required

in the present work are given below. The AXS intensities were observed at two energies of 25 and 300 eV below each absorption edge. Since the so-called EXAFS (extended x-ray absorption fine structure) and XANES (x-ray absorption near edge structure) phenomena appeared at the higher energy side of the edge make it difficult to theoretically estimate the values of anomalous dispersion terms and extremely intense fluorescent radiations disturb accurate intensity measurements, only the lower energy side was used in the present measurements. Weak fluorescent radiations of $K\alpha$ and $K\beta$, or of $L\alpha$ and $L\beta$ which mainly arise from the tail of the band pass of a monochromator crystal were observed even in the lower energy side of K- or L_{III} -absorption edge in the measurements at the energy of 25 eV below the edge. Although the $K\alpha$ or $L\alpha$ radiation can be experimentally eliminated by a solid state detector, the energy of $K\beta$ or $L\beta$ radiation is hardly separated from the elastically and incoherently scattered intensities. Thus, this $K\beta$ or $L\beta$ radiation was theoretically estimated from the observed intensity of $K\alpha$ or $L\alpha$ radiation and the tabulated intensity ratio of $K\beta$ to $K\alpha$ ¹¹⁾ or $L\beta$ to $L\alpha$ ¹²⁾ and corrected by the similar manner used in the previous works^{10,13)}. Since the incident beam intensity decays with time in a synchrotron radiation source, it was monitored with a nitrogen-gas-flow type ion-chamber placed in front of the sample¹⁴⁾. A non-negligible intensity of the higher harmonics diffracted by the Si 333 plane of the double Si crystal monochromator was observed in the present measurements. Thus, by intentionally detuning the second Si crystal of the double crystal monochromator, the intensity of the higher harmonics was reduced to the negligible level although the first order scattering intensity was also reduced to about 80% of the original intensity.

Mo $K\alpha$ radiation for the ordinary X-ray measurements were generated by a sealed Mo X-ray tube with a singly bent pyrolytic graphite monochromator in diffracted beam. Scattering intensity was observed with a scintillation detector combined with a pulse-height analyzer.

III. Data Processing

Only the fundamentals of the AXS analysis are given below, while the details may be found, e.g. in refs.10 and 13. On the lower energy side of the edge of a specific element A, the detected variation in intensity is attributed only to the change of the real part of the anomalous dispersion term f' of A. Thus, the difference between the scattering intensities measured at two energies E_1 and E_2 ($E_1 < E_2$) is

given by:

$$\begin{aligned} \Delta I_A(Q) &= I(Q, E_1) - I(Q, E_2) \\ &= c_A(f'_A(E_1) - f'_A(E_2)) \\ &\times \int_0^{Q_{\max}} 4\pi r^2 \sum_{j=1}^N \operatorname{Re}[f_j(Q, E_1) + f_j(Q, E_2)] (\rho_{Aj}(r) - \rho_{0j}) \frac{\sin(Qr)}{Qr} dr, \end{aligned} \quad (1)$$

where

$$I(Q, E_j) = I_{\text{eu}}^{\text{coh}}(Q) - \langle f^2 \rangle, \quad (2)$$

and

$$\langle f^2 \rangle = \sum_{j=1}^N c_j f_j^2. \quad (3)$$

where Q is the wave vector, and c_j and f_j are the atomic fraction and the X-ray atomic scattering factor of the j th element, respectively. Q_{\max} is the maximum value of Q used for the measurement. N is the number of constituent elements in a sample, $\rho_{Aj}(r)$ the number density function of the j th element around the element A, and ρ_{0j} the average number density for the j th element. "Re" indicates the real part of the function in the braces. For X-ray atomic scattering factors, the values tabulated in the International Tables for X-ray Crystallography, Vol. IV¹⁵) were used and for the anomalous dispersion terms the theoretical values¹⁶) computed by Cromer and Liberman's method¹⁷) were used.

The environmental radial distribution function (RDF) for A was determined by the Fourier transform of the quantity $Q\Delta I_A(Q)$:

$$\begin{aligned} 4\pi r^2 \rho_A(r) &= 4\pi r^2 \rho_0 \\ &+ \frac{2r}{\pi} \int_0^{Q_{\max}} \frac{Q\Delta I_A(Q) \sin(Qr)}{c_A(f'_A(E_1) - f'_A(E_2)) W(Q)} dQ, \end{aligned} \quad (4)$$

and

$$W(Q) = \sum_{j=1}^N c_j (f_j(Q, E_1) + f_j(Q, E_2)), \quad (5)$$

where $\rho_A(r)$ is the number density function around A and ρ_0 the average number density.

On the other hand, scattering intensity measured with the Mo K α radiation was used to estimate the ordinary RDF which represents the average structure of a sample. The measured intensity is corrected for the absorption, polarization and Compton scattering, and convert-

ed to the absolute units¹⁸⁾:

$$I_{\text{eu}}^{\text{coh}}(Q) = \langle f^2 \rangle + \langle f \rangle^2 \int_0^{Q_{\text{max}}} 4\pi r^2 (\rho(r) - \rho_0) \frac{\sin(Qr)}{Qr} dr, \quad (6)$$

and

$$\langle f \rangle = \sum_{j=1}^N c_j f_j, \quad (7)$$

where $\rho(r)$ is the average number density function. The Fourier transform of the intensity in (6) gives the ordinary RDF of the system, i.e.

$$4\pi r^2 \rho(r) = 4\pi r^2 \rho_0 + \frac{2r}{\pi} \int_0^{Q_{\text{max}}} \frac{Q [I_{\text{eu}}^{\text{coh}}(Q) - \langle f^2 \rangle]}{\langle f \rangle^2} \sin(Qr) dQ. \quad (8)$$

By comparing the environmental RDF around A in (4) with the ordinary RDF in (8), the merit of the AXS method is easily recognized. Six partial RDFs overlapped in the ordinary RDF are reduced to only three partial RDFs for pairs including the element corresponding to an absorption edge in the environmental RDF.

IV. Results and Discussion

Icosahedral $\text{Al}_{65}\text{Cu}_{20}\text{TM}_{15}$ (TM=Fe, Ru and Os) alloys

Scattering intensity profiles of the fully annealed icosahedral $\text{Al}_{65}\text{Cu}_{20}\text{TM}_{15}$ (TM=Fe, Ru and Os) alloys are shown in Fig.1¹⁹⁾. Peaks were indexed with the indexing scheme by Elser²⁰⁾, which leads lattice constants of the icosahedral $\text{Al}_{65}\text{Cu}_{20}\text{TM}_{15}$ (TM=Fe, Ru and Os) alloys to be 0.446, 0.448 and 0.452 nm, respectively. According to Elser²⁰⁾, these lattice constants correspond to the rhombohedral edge length of the three dimensional Penrose tiling. Increase in the lattice constant with atomic numbers of the element TM is qualitatively understood by increase in the atomic size of the element TM. The peak labeled "x" in Fig.1 between 111000 and 111100 peaks characterizes a new type of icosahedral phase which is distinct to the Al-Mn-Si type quasicrystals. Although its absolute intensity increases with the atomic number of TM, the amounts of increase in its intensity show a different tendency from the other indexed peaks. It is, for example, clearly seen by comparing the variations of the three peaks of 111000, "x" and 111100 in the three icosahedral alloys in Fig.1. This implies that this "x" peak is attributed to an origin completely different from that of the others. Hiraga et al.²¹⁾ interpreted

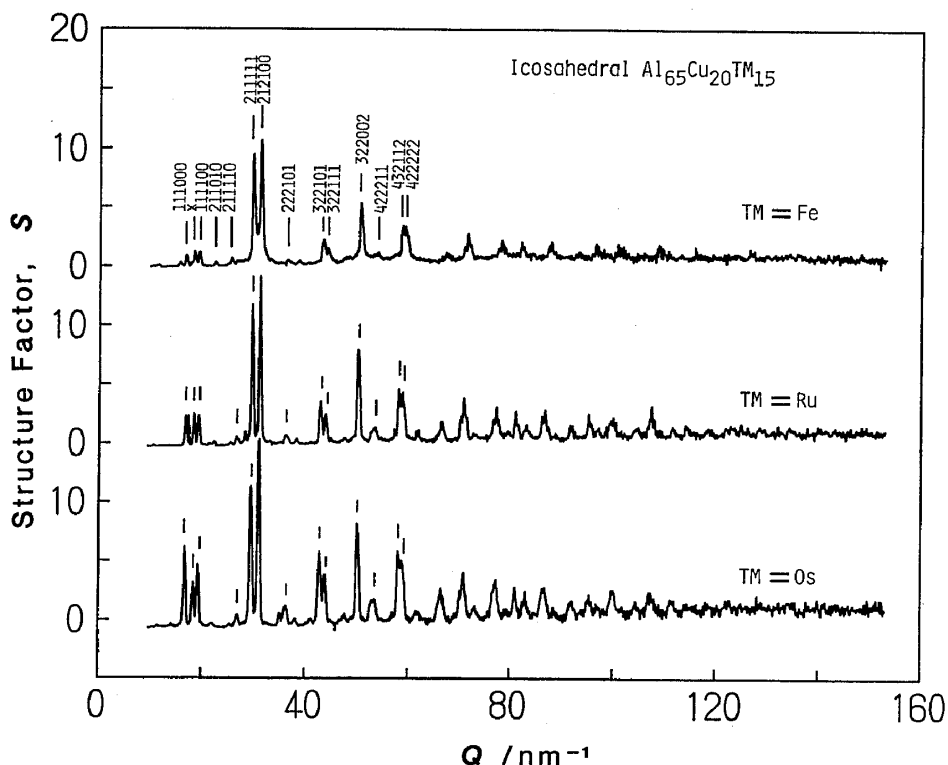


Fig.1 Structure factors of fully annealed icosahedral $\text{Al}_{65}\text{Cu}_{20}\text{Fe}_{15}$, $\text{Al}_{65}\text{Cu}_{20}\text{Ru}_{15}$ and $\text{Al}_{65}\text{Cu}_{20}\text{Os}_{15}$ alloys measured with Mo $K\alpha$ radiation¹⁹⁾. Peaks are indexed by the indexing scheme by Elser²⁰⁾.

this peak as the order-disorder transition from the face-centered six-dimensional hypercubic lattice (F-type) to the primitive six-dimensional hypercubic lattice (P-type) quasicrystal and defined as the superlattice reflection peak. Such superlattice peaks have also been observed in the icosahedral Al-Cu-Mn alloys²²⁾. However, this has not been well characterized yet in a quantitative manner. The radial distribution functions (RDFs) of the annealed icosahedral $\text{Al}_{65}\text{Cu}_{20}\text{TM}_{15}$ alloys computed in (8) are shown in Fig.2¹⁹⁾. Peaks labeled "a" to "f" in Fig.2 are detected in almost identical atomic distances in three alloys. This suggests that fundamental atomic arrangements may not be changed by replacing entire Fe atoms with Ru or Os atoms in the same column of the periodic table. The relative heights of these peaks increase with the atomic number of the element TM, which is qualitatively understood by increasing in x-ray scattering power of the element TM.

Scattering intensities of the annealed icosahedral $\text{Al}_{65}\text{Cu}_{20}\text{Os}_{15}$ alloy measured at 8.955 and 8.680 keV below Cu K-absorption edge and their differential intensity profile (ΔI) are shown in Fig.3¹⁹⁾.

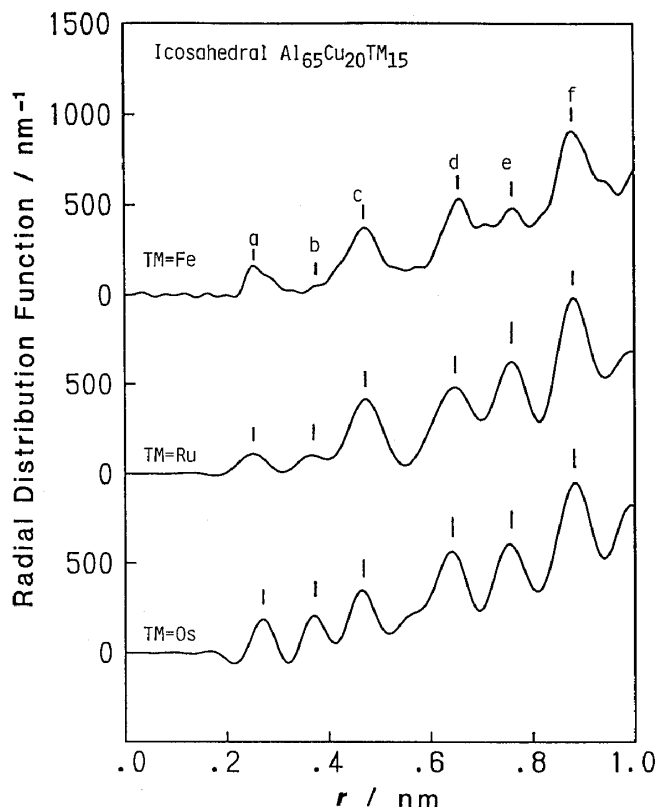


Fig.2 Radial distribution functions (RDFs) of fully annealed icosahedral $\text{Al}_{65}\text{Cu}_{20}\text{Fe}_{15}$, $\text{Al}_{65}\text{Cu}_{20}\text{Ru}_{15}$ and $\text{Al}_{65}\text{Cu}_{20}\text{Os}_{15}$ alloys measured with Mo $K\alpha$ radiation¹⁹⁾.

Both positive and negative values are observed in the differential intensity, which indicates that Cu atoms may orderly be arranged in icosahedral clusters. Similarly, scattering intensities of the icosahedral $\text{Al}_{65}\text{Cu}_{20}\text{Os}_{15}$ alloy observed at 10.844 and 8.907 keV below Os L_{III} -absorption edge and their differential intensity profile are shown in Fig.4¹⁹⁾. The differential intensity profile at Os L_{III} -absorption edge resembles the original intensity profiles in spite of a slight change of relative peak intensities in the differential profile, e.g. 211111 and 212100 at about 30 nm^{-1} in Fig.4. This is compared with the differential profile at the Cu edge in Fig.3. From these differential profiles, it is found that Os atoms are rather homogeneously dispersed in the icosahedral clusters than Cu atoms are. The same features are observed in the ordinary and environmental RDFs for Cu and Os in Fig.5¹⁹⁾. The environmental RDF for Os resembles the ordinary RDF and the environmental RDF for Cu does not. The first peak at 0.259 nm in the ordinary RDF still exists in both of the environmental RDFs for Cu and Os where the peaks are located at 0.268 and 0.270 nm, respectively. Taking account of the definition of the environmental RDF in (4) and the concentration of each element,

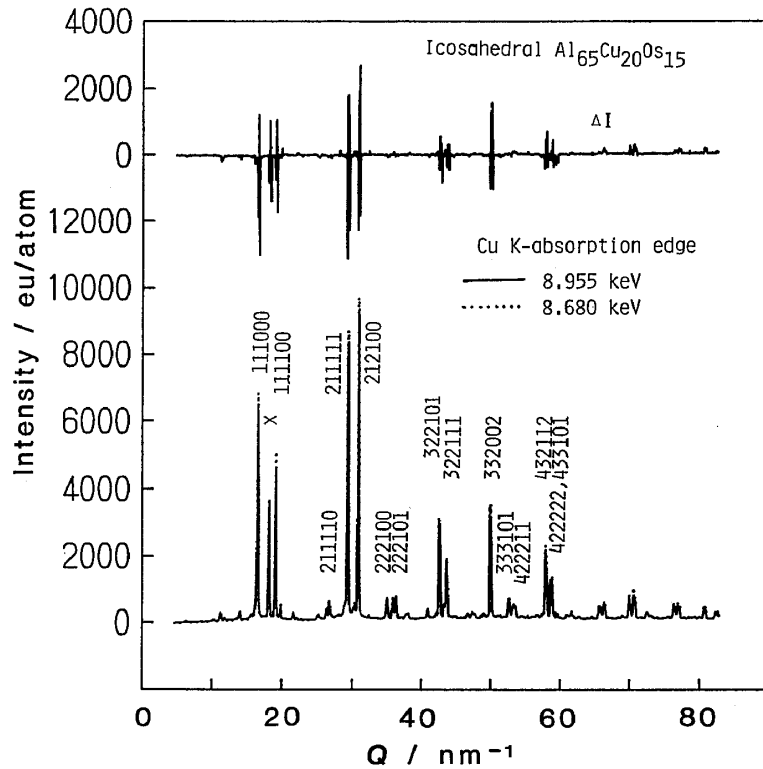


Fig.3 Differential intensity profile of fully annealed icosahedral Al₆₅Cu₂₀Os₁₅ alloy (top) defined as a difference of intensities measured at 8.955 and 8.680 keV, which are 25 and 300 eV below Cu K-absorption edge (8.980 keV)¹⁹).

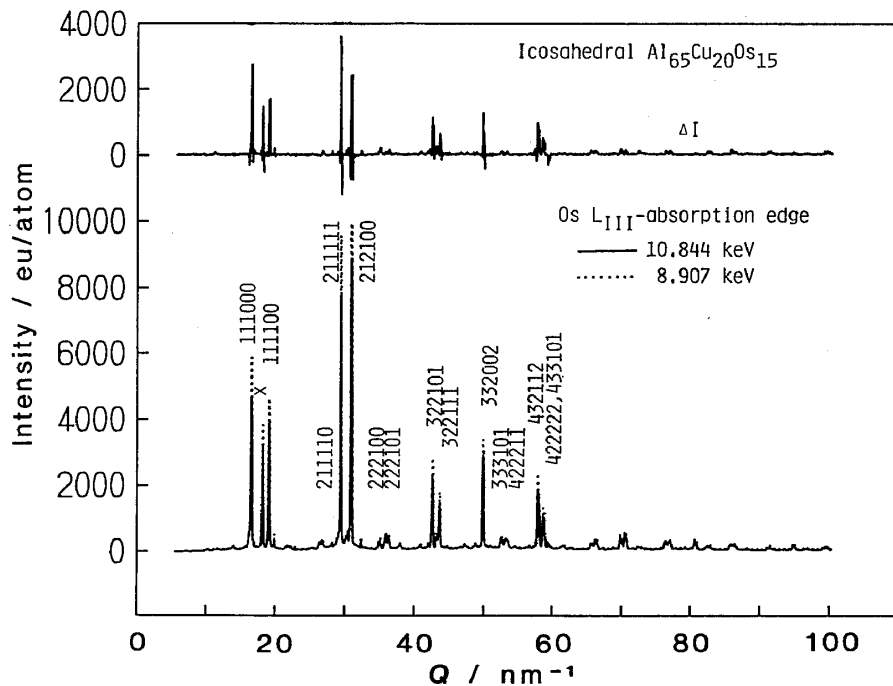


Fig.4 Differential intensity profile of fully annealed icosahedral Al₆₅Cu₂₀Os₁₅ alloy (top) defined as a difference of intensities measured at 10.844 and 8.907 keV, which are 25 and 300 eV below Os L_{III}-absorption edge¹⁹).

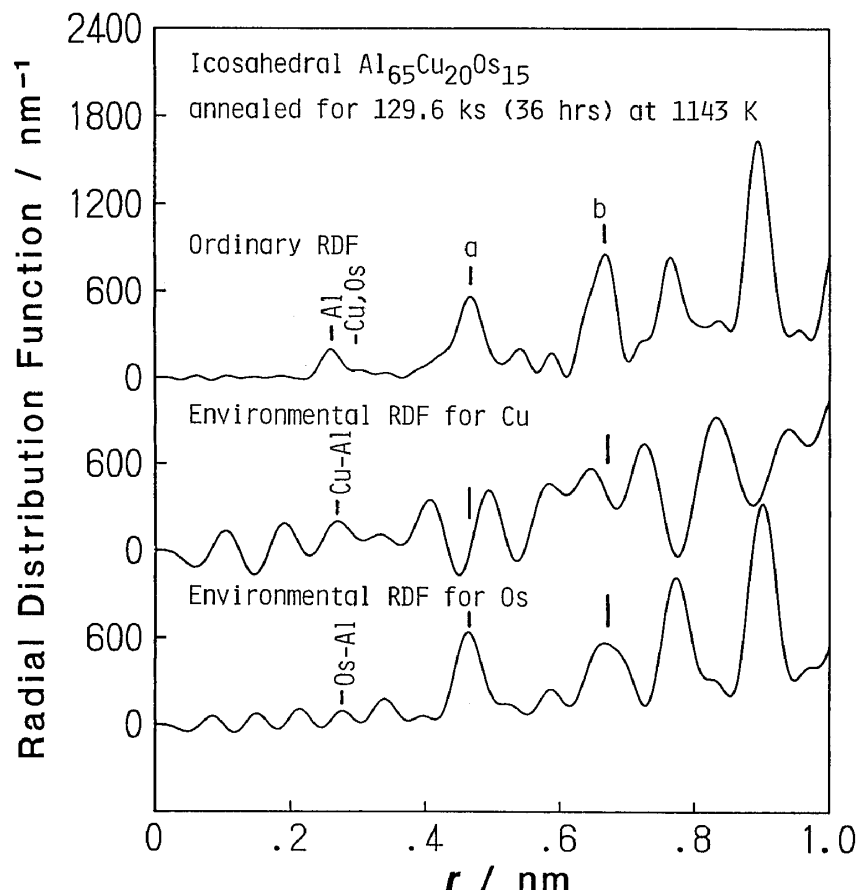


Fig.5 Ordinary radial distribution function (RDF) and environmental RDFs for Cu and Os of fully annealed icosahedral $\text{Al}_{65}\text{Cu}_{20}\text{Os}_{15}$ alloy (density= 6.457 Mg/m^3)¹⁹.

it is plausible that these peaks in the environmental RDFs for Cu and Os are attributed to Cu-Al and Os-Al pairs, respectively.

Peaks labeled "a" and "b" in Fig.5 appear at the distances of 0.463 and 0.663 nm in the ordinary RDF. Taking account of the definition of the lattice parameter (0.452 nm) in the icosahedral $\text{Al}_{65}\text{Cu}_{20}\text{Os}_{15}$ alloy, these atomic distances probably correspond to the edge and diagonal lengths of the rhombohedra of the three dimensional Penrose tiling. While there are also peaks at these distances in the environmental RDF for Os, no peak is located at these distances in the environmental RDF for Cu as seen in Fig.5. Thus, it is believed that Os atoms, not Cu atoms, occupy the vertices of the rhombohedra forming the icosahedral clusters.

Decagonal $\text{Al}_{75}\text{Fe}_{15}\text{Ni}_{10}$ alloy

Scattering intensities of the as-quenched decagonal $\text{Al}_{75}\text{Fe}_{15}\text{Ni}_{10}$ alloy measured at 7.086 and 6.811 keV below Fe K-absorption edge and their differential profile are shown in Fig.6²³). The peaks are in-

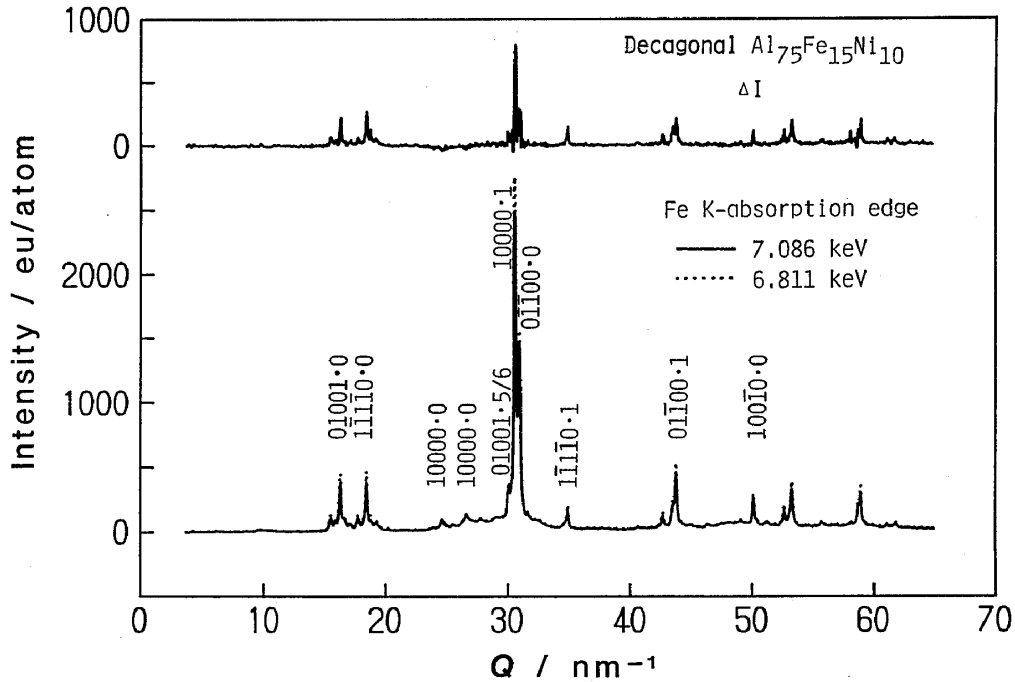


Fig.6 Differential intensity profile of as-quenched decagonal $\text{Al}_{75}\text{Fe}_{15}\text{Ni}_{10}$ alloy (top) defined as the difference of intensities measured at 7.086 and 6.811 keV²³).

dexed by the indexing scheme of the decagonal reflections proposed by Takeuchi and Kimura²⁴). Similarly, scattering intensities observed at 8.306 and 8.031 keV below Ni K-absorption edge and their difference are shown in Fig.7²³). Unlike the differential profiles at Cu K- and Os L_{III} -absorption edges in the icosahedral $\text{Al}_{65}\text{Cu}_{20}\text{Os}_{15}$ alloy in Figs.3 and 4, the two differential profiles at Fe and Ni K-absorption edges in the decagonal $\text{Al}_{75}\text{Fe}_{15}\text{Ni}_{10}$ alloy have some fundamental features in common. The two differential intensity profiles at both of the absorption edges resemble the original intensity profile, which implies that both of Fe and Ni atoms are homogeneously distributed and probably share atomic sites in the decagonal structure. This might be a reason why a single decagonal phase can be formed in a quite wide composition range, e.g. 9 to 16% Ni and 9 to 21% Fe in the ternary Al-Fe-Ni alloy⁶).

The same features in the differential profiles are also observed in the environmental RDFs for Fe and Ni in Fig.8²³). The fundamental features of the three RDFs in Fig.8 are identical. First 5 major peaks are labeled "a" to "e" in the figure. The first peak "a" in the ordinary RDF has a shoulder labeled "b" while the first peaks in the environmental RDFs for Fe and Ni have no shoulder. Taking account of the definition of the environmental RDF in (6) and the atomic concentration of each constituent element, the first peak

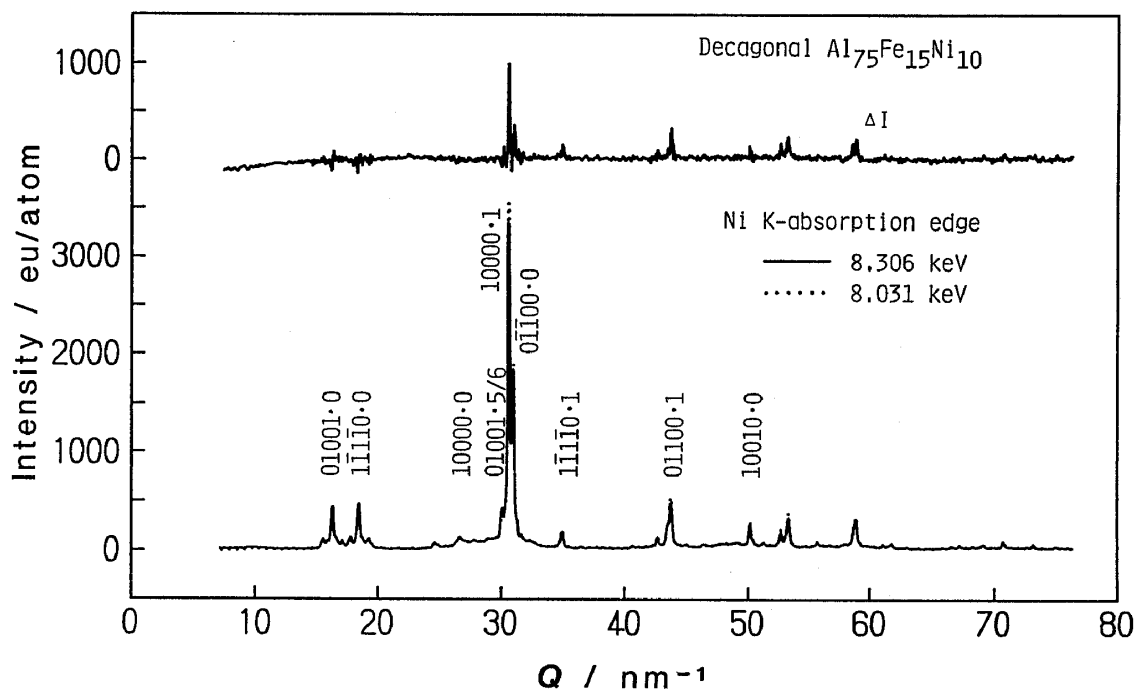


Fig.7 Differential intensity profile of as-quenched decagonal $\text{Al}_{75}\text{Fe}_{15}\text{Ni}_{10}$ alloy (top) defined as the difference of intensities measured at 8.306 and 8.031 keV²³⁾.

is attributed to the correlation of pairs of Al and transition metals and its shoulder to that of Al and Al pairs. Coordination numbers and atomic distances calculated from the first peak of the three RDFs are summarized in Table 1²³⁾. Since Fe-Al and Ni-Al pairs are located at the maximum of the first peak in the ordinary RDF, the tabulated coordination number was estimated as an average coordination number of Al atoms around Fe and Ni atoms. All of the coordination numbers computed from these three RDFs conform with each other. It is also worth noting that the atomic distances of Al-(Fe, Ni) and Al-Al pairs estimated from the ordinary RDF in Table 2 are very close to the nearest neighboring distances of Al-Fe and Al-Al pairs in $\text{Al}_{13}\text{Fe}_4$ ²⁵⁾ and their coordination numbers are roughly equal to the values of $\text{Al}_{13}\text{Fe}_4$. Henley²⁶⁾ demonstrated that the layer structure of this crystalline $\text{Al}_{13}\text{Fe}_4$ alloy can analogously be decomposed into the rhombic tiles of the two dimensional Penrose tiling. The puckered layer which is one of the two layers of the $\text{Al}_{13}\text{Fe}_4$ structure is shown in Fig.9²³⁾ with a decoration as the rhombic tiles²⁶⁾. The distances labeled "a", "b", "d" and "e" in this figure, for example, correspond to the atomic distances indicated in Fig.8. This suggests that the local atomic structure of the decagonal $\text{Al}_{75}\text{Fe}_{15}\text{Ni}_{10}$ alloy is very similar to the crystalline structure of the $\text{Al}_{13}\text{Fe}_4$ alloy. Since the atomic distances between Fe and Al atoms, or Fe and Fe

Table 1 Coordination numbers and distances in the as-quenched decagonal $\text{Al}_{75}\text{Fe}_{15}\text{Ni}_{10}$ alloy experimentally determined from the first peaks of the ordinary radial distribution function (RDF) and environmental RDFs for Fe and Ni²³⁾ with the values computed from the crystalline data of $\text{Al}_{13}\text{Fe}_4$ ²⁵⁾.

	r	N	r	N
Ordinary RDF	Fe,Ni-Al		Al-Al	
	0.252nm	7.7	0.284nm	8.6
Environmental RDF for Fe	Fe-Al			
	0.252nm	7.6		
Environmental RDF around Ni	Ni-Al			
	0.270nm	8.5		
$\text{Al}_{13}\text{Fe}_4$	0.254nm	9.7	0.279nm	7.6

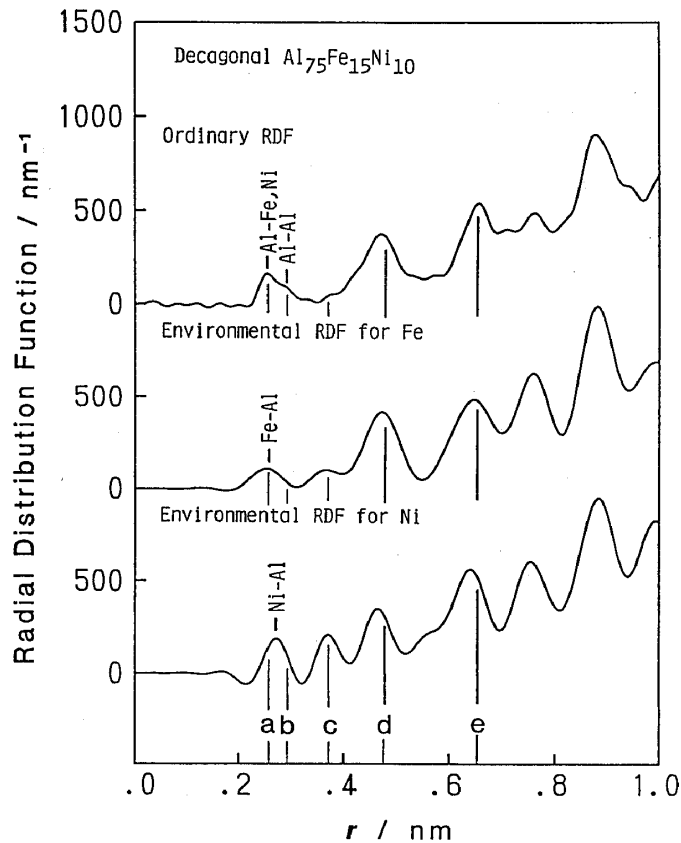


Fig.8 Ordinary radial distribution function (RDF) and environmental RDFs for Fe and Ni of as-quenched decagonal $\text{Al}_{75}\text{Fe}_{15}\text{Ni}_{10}$ alloy (density= 3.740 Mg/m^3)²³⁾.

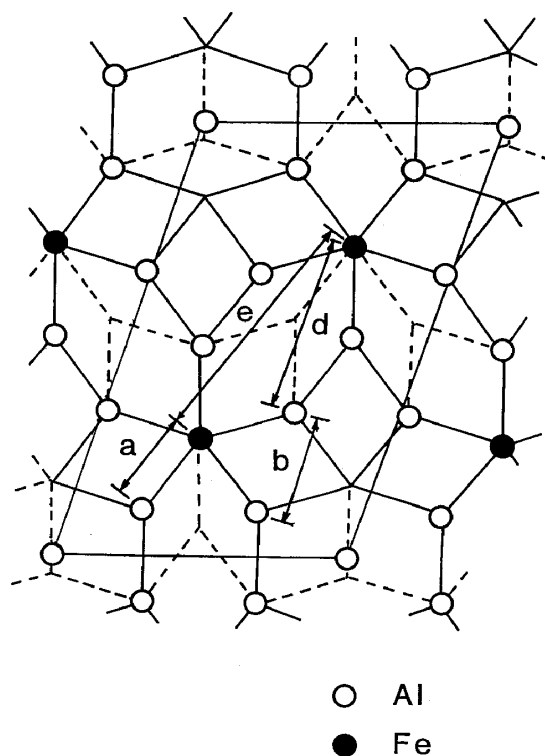


Fig.9 The puckered layer of the $\text{Al}_{13}\text{Fe}_4$ structure as a decoration of the two-dimensional Penrose tiling²⁶⁾.

atoms belonging to different layers along the c -axis in $\text{Al}_{13}\text{Fe}_4$ roughly correspond to the distance " c ", the peak labeled " c " may be attributed to some atomic arrangements perpendicular to the decagonal plane.

Edagawa et al.²⁷⁾ demonstrated that sometimes local atomic structures of icosahedral and decagonal phases are successfully approximated by some crystalline structures with very large lattice constants. Our present results in the decagonal $\text{Al}_{75}\text{Fe}_{15}\text{Ni}_{10}$ alloy by the AXS technique supports their result and the similarity of the local atomic structures between the decagonal $\text{Al}_{75}\text{Fe}_{15}\text{Ni}_{10}$ and crystalline $\text{Al}_{13}\text{Fe}_4$ alloys has been revealed.

Authors are grateful to the Ministry of Education, Science and Culture of Japan for financial support of a Grant-in-Aid for Scientific Research on Priority Areas (01630001). A part of this Research was also supported by the Science Foundation for Light Metals and Alloys. All the samples used in the present measurements are provided by Dr. Tsai, and Profs. Inoue and Masumoto in Institute for Materials Research, Tohoku University.

References

- (1) A.P.Tsai, A.Inoue and T.Masumoto, Japanese J.Appl.Phys., **26** (1987), L1505.
- (2) A.P.Tsai, A.Inoue and T.Masumoto, J.Mater.Sci.Lett., **7** (1988), 322.
- (3) A.P.Tsai, A.Inoue and T.Masumoto, Japanese J.Appl.Phys., **27**, (1988), L1587.
- (4) E.Matsubara, Y.Waseda, A.P.Tsai, A.Inoue and T.Masumoto, Z.Naturforsch., **45a** (1990), 50.
- (5) C.L.Henley, Comments on Condensed Matter Physics, **13** (1987), 59.
- (6) A.P.Tsai, A.Inoue and T.Masumoto, Mat.Trans.Japan.Inst.Metals, **30**(1989), 150.
- (7) A.P.Tsai, A.Inoue and T.Masumoto, *ibid.*, **30** (1989), 300.
- (8) C.L.Henley, Physica, **140A** (1986), 306.
- (9) M.Audier and P.Guyot, Phil.Mag.B, **53** (1986), L43.
- (10) E.Matsubara, K.Harada, Y.Waseda and M.Iwase, Z.Naturforsch., **43a** (1988), 181.
- (11) N.V.Rao, S.B.Reddy, G.Satyanarayana and D.L.Sastry, Physica, **138c**(1986), 215.
- (12) B.K.Teo, *EXAFS: Basic Principles and Data Analysis*, Springer-Verlag, New York (1986), 9.
- (13) S.Aur, D.Kofalt, Y.Waseda, T.Egami, R.Wang, H.S.Chen, and B.K.Teo, Solid State Commun. **48** (1983), 111.
- (14) E.Matsubara, Y.Waseda, M.Mitera and T.Masumoto, Trans.Japan.Inst.Met., **29** (1988), 697.
- (15) *International Tables for X-ray Crystallography, Vol.IV*, (Kynoch, Birmingham, 1974) p.148.
- (16) Y.Waseda, *Novel Application of Anomalous X-ray Scattering for Structural Characterization of Disordered Materials*, Springer-Verlag, New York (1984) p.84.
- (17) D.T.Cromer and D.Liberman, J.Chem.Phys., **53** (1970), 1891.
- (18) Y.Waseda, *Structure of Non-Crystalline Materials*, McGraw-Hill, New York, (1980) p.60.
- (19) E.Matsubara, Y.Waseda, A.P.Tsai, A.Inoue, T.Masumoto, in preparation.
- (20) V.Elser, Phys.Rev.B, **32** (1985), 4892.
- (21) K.Hiraga, M.Hirabayashi, A.P.Tsai, A.Inoue and T.Masumoto, Phil.Mag.Lett., **60** (1989), 201.
- (22) S.Ebalard and F.Spaepen, J.Mater.Res., **4** (1989), 43.
- (23) E.Matsubara, Y.Waseda, A.P.Tsai, A.Inoue, T.Masumoto, in preparation.
- (24) S.Takeuchi and K.Kimura, J.Phys.Soc.Japan, **56** (1987), 982.
- (25) P.J.Black, Acta Cryst., **8** (1955), 175.
- (26) C.L.Henley, J.Non-Cryst.Solids, **75** (1985), 91.
- (27) K.Edagawa, K.Suzuki, M.Ichihara, S.Takeuchi and T.Shibuya, Phil.Mag.B, to be submitted.